Journal of
MECHANICAL and ENERGY
ENGINEERING

ISSN: 2544-0780 | e-ISSN: 2544-1671
Vol. 5(45) | No. 2| June 2021 | pp. 103-112
DOI: 10.30464/jmee.2021.5.2.103

PREDICTING PROCESS PARAMETERS ON WELD NUGGET HARDNESS OF FILLER ADDED FRICTION STIR WELDED DISSIMILAR ALUMINIUM ALLOYS 5052 AND 6082 JOINTS

A. SASIKUMAR[1], S. GOPI[1], Dhanesh G. MOHAN[2*]

[1]Department of Production Engineering, Government College of Technology, Coimbatore, Tamilnadu, India
[2*]Institute of Materials Joining, Shandong University, Jinan, China, email: dhaneshgm@gmail.com

(Received 18 June 2021, Accepted 30 June 2021)

Abstract: This article deals with the optimization of friction stir welding process parameters with filler ratios on dissimilar aluminium alloy groups. For this purpose, 6 series aluminium alloy 6082 and 5 series aluminium alloy 5052 were taken. Microhardness property investigation was conducted under various rotational speeds, welding speed, plunge depth, center distance between the holes and the filler mixing ratio. The Central Composite Design (CCD), the most commonly used Response Surface Methodology (RSM), is considered to develop the prediction equation. A validation analysis is carried out, and the results were compared with the relative impact of input parameters on weld nugget microhardness. It is observed that the increase in welding speed with the plunge depth and the filler ratio result in an increase of weld nugget microhardness up to a maximum value. The maximum weld nugget hardness of the joint fabricated was obtained with the welding process parameters combination of 1000 rpm rotational speed, 125 mm/min welding speed, 0.15 mm plunge depth, 2 mm centre distance between the holes, and the filler ratio of 95% Mg and 5% Cr.

Keywords: friction stir welding, center distance between holes, filler ratio, microhardness, response surface methodology

1. INTRODUCTION

The Friction Stir Welding (FSW) process possesses a non-consumable rotating tool to perform the weld. The rotating tool comprises a shoulder and a pin. The shape and size of the tool shoulder and pin improve the heat generation and, in turn, it improves the plastic flow in the welding region of the workpiece. The plasticization and solidification of the weld joints cause in a change of mechanical and microstructural properties, such as tensile strength, the hardness of the weld, ductility and corrosion behaviour. The plastic deformation of the parent metal while welding resulting in a fine grain structure is due to the shearing action of the rotating pin and the forging action of the shoulder [1]. The microhardness of the friction stir zone is always comparatively lesser than that of the base metal due to the structural deformation in the welding region. Hence, an attempt was made to improve the mechanical properties of the joint by introducing a filler material in between the joint during welding [2]. The investigation is carried out on dissimilar material joints of AA6082 and AA5052 by friction stir welding. AA5052 (Al-Mg) is mainly used in marine areas, building construction and food processing industries due to its natural corrosion resistance property. AA6082 (Al-Mg-Si) is widely used in marine structural frames due to its high joint strength, and the FSW technique improves the joint strength of dissimilar aluminium 5xxx and 6xxx alloys [3].

RSM was employed to develop the regression models and to predict the responses. RSM is to predict the optimum process parameters with the maximum weld nugget hardness. RSM predicts the following process parameters to be the best: 1100 rpm tool rotational speed, 80 mm/min welding speed, 8 kN axial force, with the tool parameters of 15 mm shoulder diameter, 5 mm pin diameter and 45 HRC

tool hardness [4]. A mathematical model with process parameters and tool geometry predicts the responses of friction stir welds of AA2014-T6 aluminium alloy and optimizing the process parameters to obtain a higher joint strength for friction stir welded 6082-T6 aluminium alloy. The tool rotation plays a dynamic role in FSW. The friction stir welded AA6082 joint shows better strength while increasing the tool rotation between 700 rpm and 900 rpm. The strength of the joint is decreased gradually after an increase of spindle speed between 1100 rpm and 1500 rpm. Better joint strength is achieved at 900 rpm. The increase in the shoulder penetration while welding AA6082 increases microhardness. The maximum microhardness is achieved by 0.08 mm of the shoulder penetration of the hexagonal pin profile. The weld nugget zone exposed higher weld hardness than the base metals due to the dynamic recrystallization of metals [5].

2. EXPERIMENTAL PROCEDURE

The experimental process parameters such as rotational speed, welding speed, plunge depth, the centre distance between holes and filler mixing ratio were considered. After many trials, the rotational speed and the welding speed range were accepted to range from 600 rpm to 1400 rpm and 60 mm/min to 180 mm/min, respectively. The plunge depth was gradually increased in five steps of 0.05 mm from 0 mm to 0.25 mm. Along the butting surface of the weld specimen, the holes were drilled having dimensions of 2 mm in diameter, 3 mm in depth, and the filler holes centre distance was maintained in a zig zag position. The ranges were accepted to be from 0 mm to 4 mm. The centre distance between the holes in zig zag positions are 0 mm, 1 mm, 2 mm, 3 mm and 4 mm respectively. The process parameters with their ranges and values are tabulated in Table 1.

Tab. 1. Process parameters with their ranges and values at five levels

Parameters	Notation with unit	Parameter levels
		(-2) (-1) (0) (1) (2)
Rotational speed	R, rpm	600 800 1000 1200 1400
Welding speed	W, mm/min	60 90 120 150 180
Plunge depth	P, mm	0.05 0.1 0.15 0.2 0.25
Center distance between the holes	C, mm	0 1 2 3 4
Filler ratio (Mg: Cr)	F, %	90: 92.5: 95: 97.5: 100: 10 7.25 5 2.5 0

The magnesium (Mg) and chromium (Cr) powders were selected as filling agents to join the alloy plates of AA5052 and AA6082. Magnesium promotes mechanical properties of the weld joint, and chromium improves corrosion resistance property and microhardness. The average weight percentage of Mg and Cr was determined in the weld stir zone. The weight percentage ratio was calculated from the average weight percentage of Mg and Cr in the weld stir zone. The weight percentage ratio of Mg and Cr fillers were calculated from the total weight of the filler. The weight percentage of Mg and Cr filler mixing ratios were maintained at 90:10, 92.5:7.5, 95:5, 97.5:2.5 and 100:0 [6]. This work used a tool shoulder diameter of 20 mm, a pin length of 7.6 mm, and a hexagonal profile pin diameter of 8 mm. The weld base metals' chemical compositions and mechanical properties are tabulated in Tables 2 and 3, respectively.

Tab. 2. Chemical composition (wt.%) of AA5052 and AA6082

Alloy elements	Weight percentage	
	AA5052	AA6082
Magnesium	2.629	0.82
Silicon	0.049	1.0
Chromium	0.196	0.05
Manganese	0.016	0.52
Ferrous	0.186	0.27
Copper	0.006	0.02
Zinc	0.009	0.1
Nickel	0.04	–
Titanium	0.016	0.03

Tab. 3. Physical and Mechanical Properties of AA5052 and AA6082

Density (g/cm^3)	2.680	2.700
Melting point (°C)	607	555
Ultimate tensile strength (MPa)	217	330
Yield strength (MPa)	168	279
Elongation (%)	19.5	13
Vickers hardness (HV)	85	120
Aluminium	Balance	Balance

Aluminium alloy 5052 and 6082 of 8 mm thick plates were used as the base metal. The base metal plates were prepared in 150 mm × 75 mm dimensions. Aluminium alloy 6082 provides better tensile strength, and aluminium alloy 5052 reveals better corrosion resistance properties. The square butt joint structure

was prepared to fabricate FSW joints. The drilled holes were aligned in a zig-zag position for conducting FSW. The schematic diagram of a joint configuration in detail is shown in Figure 1.

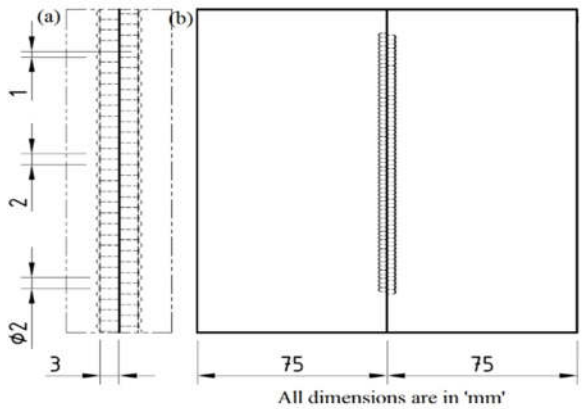

Fig. 1. Schematic diagram of FSW in detail a) enlarged view of zig-zag hole position, b) schematic diagram of weld specimen

Aluminium alloy 5052 plate was placed on the advancing side and 6082 plate on the retreating side. High heat and wear-resistant tools made of tungsten carbide were used to fabricate the weld joints. The tool geometry with a hexagonal pin profile is shown in Figure 2. The HMT FN2V vertical milling machine with 7.5 Hp and 1800 rpm is used for FSW operation.

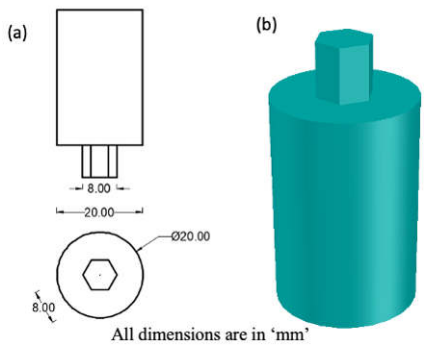

Fig. 2. Design of FSW tool a) tool geometry b) model of the hexagonal pin profile

3. RESULTS AND DISCUSSIONS

Response Surface Methodology (RSM) is a mathematical and statistical technique. It is used for analyzing problems in which several independent variables influence a dependent variable or response. The aim is to optimize the process parameters and to enhance the responses. In various experimental conditions, it represents an independent factor in a quantitative form as given in Eq. (1). The variables (x_1, x_2, x_3... x_k of k quantitative factors) can be formed as a response or functional relationship (Y) as follows [7].

$$Y = \varphi\,(x1, x2 \ldots xk) \pm er. \quad (1)$$

The response function is represented as φ. The residual er is the measure of experimental errors. The characteristic is responding to a given set of independent variables. When the mathematical form of φ is unknown, a polynomial can approximate satisfactorily within the experimental region. In the present investigation, the RSM was applied to develop the mathematical model in the form of regression equations for the quantitative characteristics of the friction stir welded AA5052 and AA6082 alloys. Applying the RSM, the independent variable was viewed as a surface to which a mathematical variable is fitted. The microhardness of the joints represent MH. The response is a function of rotational speed (R), welding speed (W), plunge depth (P), the centre distance between the holes (C), and filler ratio (F), and it can be expressed in Eq. (2):

$$MH = f\,(R, W, P, C, F). \quad (2)$$

The second-order polynomial (regression equation) used to represent the response surface 'Y' is given in Eq. (3)"

$$Y = bo + \Sigma\, bixi + \Sigma\, biixi2 + \\ + \Sigma\, bijxixj + er. \quad (3)$$

The relationship between the responses with factors is represented in Eq. (4):

$$MH = bo + b1(R) + b2(W) + \\ + b3(P) + b4(C) + b5F) + \\ + b11(R2) + b22(W\,2) + b33(P2) + \\ + b44(C2) + b55(F2) + b12(RW) + \\ + b13(RP) + b14(RC) + b15(RF) + \\ + b23(WP) + b24(WC) + b25(WF) + \\ + b34(PC) + b35(PF) + b45(CF). \quad (4)$$

Where b_o is the average of responses and b_1, b_2…, b_{45} are coefficients that depend on respective primary, square and interaction effects of factors. A decision was taken to use, in the range of the parameters, five factors, five levels, central composite design matrix to optimize the experimental conditions. Table 4 shows the half factorial design that has derived 32 sets of code conditions used to form the design matrix. The first 26 coded experimental conditions have a non-centred level and are centred for the last 6 experiments. These 32 experimental conditions allowed an estimation of the variables linear, quadratic and two-way interactive effects on the microhardness of the joints welded.

3.1. Hardness testing

A Vickers's microhardness testing machine (Make: Mitutoyo and Model: HM200) shown in

Figure 3 was employed to measure the weld zones hardness with 0.05 kg load at 15 s. The specimens for the hardness inspection were sectioned to the required sizes from the joint FSZ, TMAZ, HAZ and base metal regions. The surfaces were polished using different grades (300#, 500#, 800# and 1200#) of SiC emery papers. The microhardness test was conducted for thirty-two FSW specimens, and the results were tabulated in Table 4. The impact of the process parameters on the microhardness of AA6082 and AA5052 dissimilar alloy is shown in Figure 4.

Table 5 shows the ANOVA test results for the microhardness. The Model F-value of 84.15 denotes that the model is significant. There is only a 0.01% chance that an F-value that is large like this could occur due to noise. P-values less than 0.05 specify that model terms are significant.

Fig. 3. Vickers's microhardness testing machine

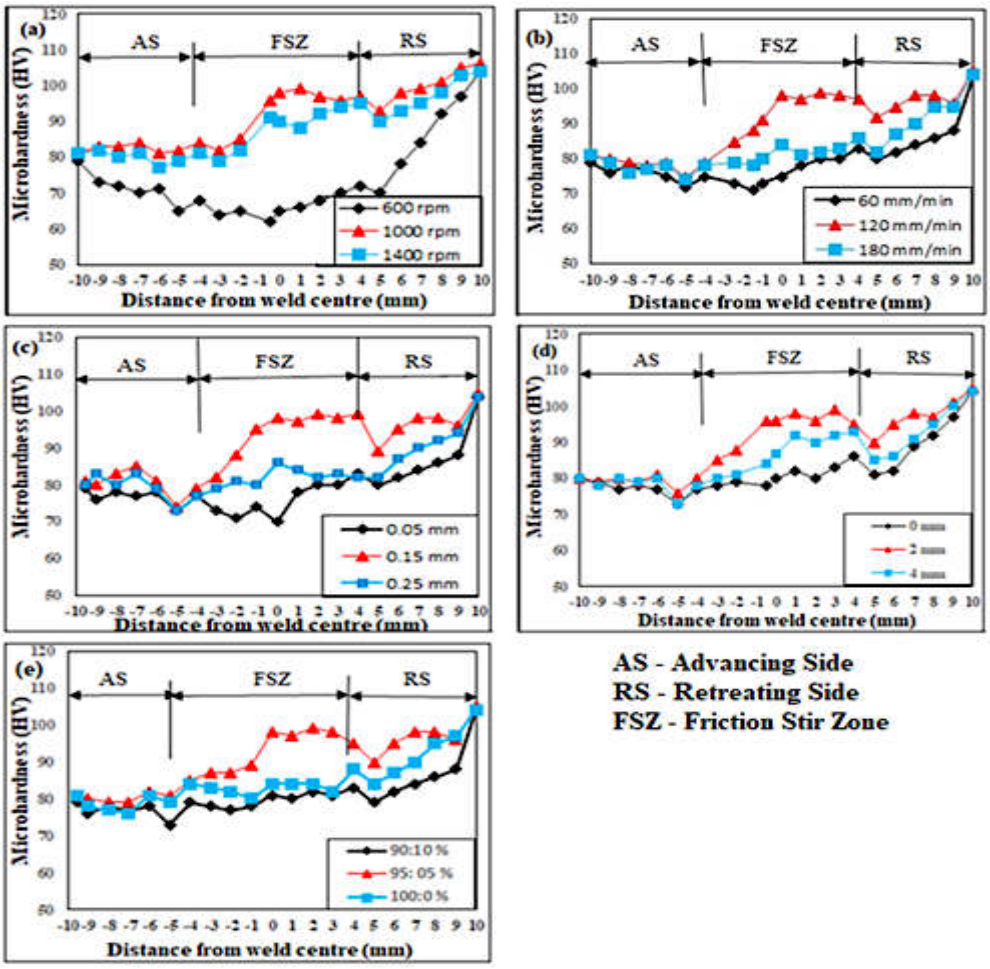

Fig. 4. Effect of process parameters on the microhardness of AA6082 and AA5052 dissimilar alloy: a) rotational speed, b) welding speed, c) plunge depth, d) center distance between the holes, e) filler mixing ratio

Tab. 4. Design matrix for Microhardness

						Result
Exp.no	Input parameters					Response
	R, rpm	*W*, mm/min	*P*, mm	*C*, mm	*F*, %	*MH*, HV
1.	800	90	0.1	1	97.5:2.5	66
2.	1200	90	0.1	1	92.5:7.5	69
3.	800	150	0.1	1	92.5:7.5	68
4.	1200	150	0.1	1	97.5:2.5	84
5.	800	90	0.2	1	92.5:7.5	67
6.	1200	90	0.2	1	97.5:2.5	85
7.	800	150	0.2	1	97. 5:2.5	70
8.	1200	150	0.2	1	92.5:7.5	85
9.	800	90	0.1	3	92.5:7.5	70
10.	1200	90	0.1	3	97.5:2.5	84
11.	800	150	0.1	3	97.5:2.5	75
12.	1200	150	0.1	3	92.5:7.5	85
13.	800	90	0.2	3	97.5:2.5	74
14.	1200	90	0.2	3	92.5:7.5	86
15.	800	150	0.2	3	92.5:7.5	73
16.	1200	150	0.2	3	97.5:2.5	86
17.	600	120	0.15	2	95.0:5.0	65
18.	1400	120	0.15	2	95.0:5.0	88
19.	1000	60	0.15	2	95.0:5.0	75
20.	1000	180	0.15	2	95.0:5.0	81
21.	1000	120	0.05	2	95.0:5.0	76
22.	1000	120	0.25	2	95.0:5.0	82
23.	1000	120	0.15	0	95.0:5.0	80
24.	1000	120	0.15	4	95.0:5.0	86
25.	1000	120	0.15	2	90.0:10.0	79
26.	1000	120	0.15	2	100.0:0.0	83
27.	1000	120	0.15	2	95.0:5.0	93
28.	1000	120	0.15	2	95.0:5.0	93
29.	1000	120	0.15	2	95.0:5.0	92
30.	1000	120	0.15	2	95.0:5.0	91
31.	1000	120	0.15	2	95.0:5.0	93
32.	1000	120	0.15	2	95.0:5.0	90

Tab. 5. ANOVA test results for Microhardness

Source	Sum of Squares	Degree of freedom	Mean Square	F-value	p-value	
Model	2350.51	20	117.53	84.15	< 0.0001	Significant
*R**	900.38	1	900.38	644.65	< 0.0001	
*W**	57.04	1	57.04	40.84	< 0.0001	
*P**	57.04	1	57.04	40.84	< 0.0001	
*C**	108.38	1	108.38	77.59	< 0.0001	
*F**	35.04	1	35.04	25.09	0.0004	
RW	3.06	1	3.06	2.19	0.1667	
*RP**	14.06	1	14.06	10.07	0.0089	
RC	0.5625	1	0.5625	0.4027	0.5387	
RF	3.06	1	3.06	2.19	0.1667	
*WP**	27.56	1	27.56	19.73	0.001	
*WC**	14.06	1	14.06	10.07	0.0089	
*WF**	10.56	1	10.56	7.56	0.0189	
*PC**	14.06	1	14.06	10.07	0.0089	
*PF**	10.56	1	10.56	7.56	0.0189	
*CF**	7.56	1	7.56	5.41	0.0401	
R^2*	427.64	1	427.64	306.18	< 0.0001	
W^2*	347.76	1	347.76	248.99	< 0.0001	
P^2*	299.09	1	299.09	214.14	< 0.0001	
C^2*	141.09	1	141.09	101.02	< 0.0001	
F^{2*}	212.76	1	212.76	152.33	< 0.0001	
Residual	15.36	11	1.4			
Lack of Fit	7.36	6	1.23	0.767	0.6267	Not significant
Pure Error	8	5	1.6			
Cor Total	2365.88	31				
Std deviation	1.18		R^2	0.9935		
Mean	80.44		Adjusted R^2	0.9817		
CV, %	1.47		Predicted R^2	0.9124		
PRESS	207.14		Adeq. Precision	28.7479		

*Significant

In this case, *R, W, P, C, F, RP, WP, WC, WF, PC, PF, CF,* R^2, W^2, P^2, C^2, F^2 is significant model terms. The final empirical relationships to evaluate the microhardness of the weld region are represented in Eq. (5).

$$MH = 91.94 + 6.13(R) + 1.54(W) + 1.54\,(P) + 2.13\,(C) + 1.21(F) + +0.9375(RP) - 1.31(WP) - 0.9375(WC) - 0.8125(WF) - 0.9375(PC) - 0.8125(PF) - - 0.6875(CF) - 3.82(R^2) - 3.44(W^2) - - 3.19(P^2) - 2.19(C^2) - 2.69(F^2) HV. \quad (5)$$

The Lack of the Fit F-value of 0.767 implies the Lack of Fit is not significant relative to the pure error. There is a 62.67% chance that the Lack of the Fit F-value that is of this quantity could occur due to noise. The Predicted R^2 of 0.9124 is in reasonable agreement with the Adjusted R^2 of 0.9817 because the difference is less than 0.2. Adequate Precision is used to measures the signal to noise ratio. A ratio greater than 4 is desirable. In this model, 28.7479 specifies an adequate signal. The predicted versus actual response plot for the microhardness is shown in Fig. 5. From this plot, experimental response values are compared with the predicted response values calculated from the ANOVA model.

The perturbation plot is used to compare the effect of all the process parameters at a particular point in the design space. It is observed that the weld nugget hardness is maximum as the tool rotational speed is at the central level, whereas the tool rotational speed increases with increased microhardness significantly, as shown in Fig. 6.

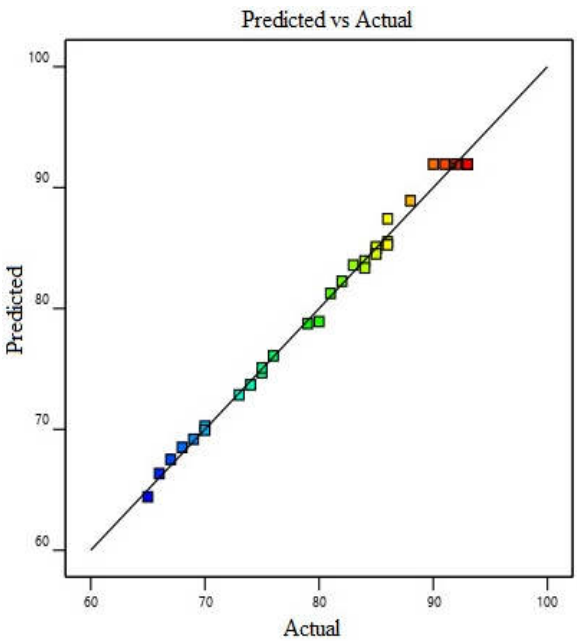

Fig. 5. Predicted vs actual response for microhardness

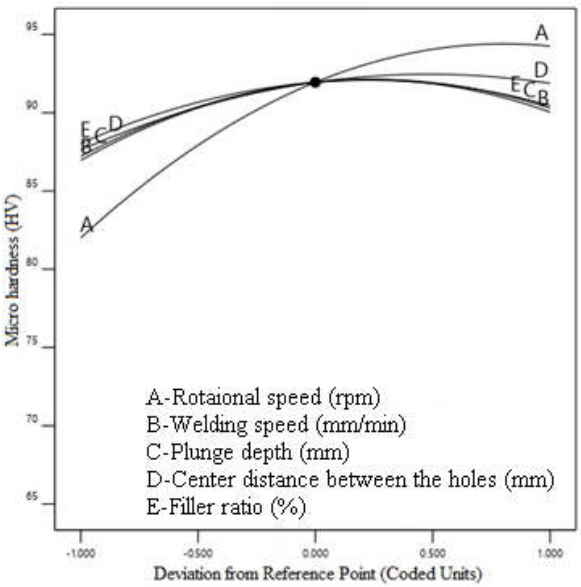

Fig. 6. Perturbation plot showing the effect of all factors on the microhardness

4. RESPONSE OPTIMIZATION

The challenge for the manufacturer is how to select the process parameters that would produce a better-welded joint. Usually, defining the process parameters for new welded products to produce a welded joint with the required specifications is a time-consuming trial accompanied by an error development effort. The welding process parameters were selected by the skill of the engineer or the machine operator. Then, the weld is inspected to determine whether it meets the requirement or not. Finally, the selected process parameters would produce a welded joint near the required specification. Also, it is not considered to attain the optimized welding parameter combinations. The welding process parameters can be predicted precisely without consuming time and labour effort by using various model development methods. The first objective is to employ RSM to relate the FSW input parameters (the tool rotational speed, the welding speed, the plunge depth, the centre distance between the holes and the powder mixing ratio) to the output response (microhardness). The second objective is to find the optimal welding input parameter combination that would maximize microhardness.

4.1. Desirability approach

There are various statistical techniques for solving multiple response problems like constrained optimization problems, overlaying the contour plot for each response, and the desirability approach. The desirability method is suggested due to its simplicity, and it is available in software. It provides flexibility in weightage and giving importance to the individual response.

The multiple response optimization problems were solved by using the technique of desirability approach. The technique for combining multiple responses into a dimensionless measure of performance is called the overall desirability function. The desirability approach involves transforming each estimated response *Yi* into a unitless utility bounded by $0 < di < 1$, where a higher *di* value indicates that response value *Yi* is more desirable if $di = 0$ means a non-preferred response.

In this research work, the desirability of response *di* was calculated using Eqs. (6). The desirability function can be changed for each goal by weightage '*wti*'. Weightage is used to give more importance to the upper/lower bounds value. The range of weightage is between 0.1 and 10. The weightage greater than 1

gives more importance to the goal, while weightage less than 1 gives less importance. When the weightage value is equal to 1, the *di* will vary from 0 to 1. In the desirability objective function (*D*), each response can be allotted importance (*r*) relative to other responses. Importance varies from the least significant value of 1, indicated by (+), to the most critical value of 5, indicated by (+++++). The overall objective function is shown in Eq. (7), where *n* is the number of the responses inspected.

For the objective of maximum, the desirability will be defined by:

$$d_i = \begin{cases} 0 & , \quad Y_i \leq Low_i \\ \left(\dfrac{y_i - Low_i}{High_i - Low_i} \right)^{wt_i} & , Low_i < Y_i < High_i \\ 1 & , \quad Y_i \geq High_i \end{cases} . \quad (6)$$

The overall objective function is defined by:

$$D = \left(\prod_{i=1}^{n} d_i^{ri} \right)^{1/\sum ri} . \quad (7)$$

4.2. Central Composite Design

Once the models have been developed and verified for adequacy, the optimization criteria can be set to find out the optimal welding process parameters conditions. In this investigation, the criteria were implemented to process parameters in the range, the tensile strength at the maximum, microhardness set to the maximum and the corrosion rate at the minimum. The optimization criteria used in this study were represented in Table 6. The optimal solution was achieved by design-expert software based on the criteria presented in Table 7.

The welding speed is one of the process parameters responsible for generating heat in the region welded. The optimum welding speed is used to produce a better plasticization of the base metal in the region welded. The combination of the optimum values of the welding speed and the powder mixing ratio produces the maximum microhardness. The optimum process parameters produced the maximum value for microhardness, viz, the welding speed of 124.952 mm/min, and the powder mixing ratio of 95.042% Mg, 4.958% Cr, as shown in Figure 7.

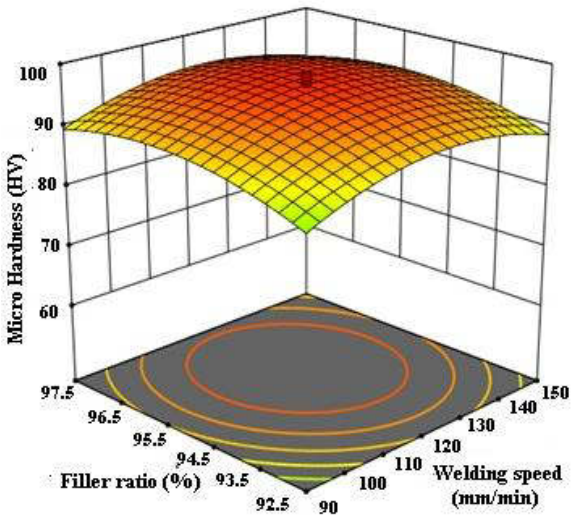

Fig. 7. 3D plot shows the effect of welding speed and filler mixing ratio on microhardness

Tab. 6. Optimization criteria used in this study

Parameters and responses	Limits		Impor-tance	Criterion
	Lower	Higher		
Rotational speed, rpm	600	1400	3	In range
Welding speed, mm/min	60	180	3	In range
Plunge depth, mm	0.05	0.25	3	In range
Center distance between the holes, mm	0	4	3	In range
Filler ratio, %	90:10	100:0	3	In range
Weld nugget hardness, HV	66	93	5	Maximize

Tab. 7. Optimal solution as obtained by design-expert software

Exp.no	Experimental details					Results	
	Input parameters					Responses	
	R (rpm)	W (mm/min)	P (mm)	C (mm)	M (%)	MH (HV)	Desirability
1	1040.862	124.931	0.157	2.062	95.043:4.957	93.4843	0.911247
2	1041.011	124.979	0.157	2.064	95.038:4.962	93.4821	0.911247
3	1040.999	124.952	0.157	2.064	95.042:4.958	93.4863	0.911247
4	1041.076	124.970	0.157	2.062	95.052:4.948	93.4852	0.911246
5	1041.111	125.022	0.157	2.063	95.052:4.948	93.4911	0.911246

4.3. Confirmation Test

Three confirmation tests were carried out with the welding parameter conditions selected randomly from the optimization results. The predicted optimum parameters for the filler added FSW based on the levels is given in Table 8. Confirmatory tests were conducted, and the microhardness was found by using optimal parameters. Due to the limitation for setting the parameters to the predicted value, the round off value is selected for the validation test.

Tab. 8. Optimum parameters for confirmation test

Rotational speed, rpm	Welding speed, mm/min	Plunge depth, mm	Center distance between the holes, mm	Filler ratio, %
1000	125	0.15	2.0	95:05

The accuracy of optimal parameters was found by conducting a confirmatory test. The predicted vs. actual value and the percentage of error for microhardness is shown in Table 9. The optimum process parameters values and average microhardness of filler added friction stir welded AA6082 and AA5052 was found 93 HV.

Tab. 9. Confirmation Test Results

Input parameters	Exp. no	Responses	
			MH (HV)
Rotational speed = 1000 rpm Welding speed = 125 mm/min Plunge depth = 0.15 mm Center distance between the holes = 2 mm Filler ratio = 95:5 %	1	Actual	89.027
		Predicted	93.4843
		Error %	4.77
	2	Actual	89.214
		Predicted	93.4821
		Error %	4.57
	3	Actual	88.708
		Predicted	93.4852
		Error %	4.61

5. CONCLUSIONS

Based on the experimental studies with an optimization of the magnesium and chromium filler in the friction stir welded dissimilar joints of AA5052 and AA6082 the following significant conclusions are drawn:

- the RSM technique is used to optimize the friction stir welding parameters to obtain the maximum weld nugget hardness,
- welding speed 125 mm/min is an optimum input parameter to obtain the maximum weld nugget hardness produced from AA6082 and AA5052 aluminium alloy,
- the interaction of the welding speed with plunge depth is the most significant factor to obtain maximum microhardness,
- the fabricated joint with a rotational speed of 1000 rpm, welding speed 125 mm/min, the plunge depth 0.15 mm, the centre distance between the filler holes 2 mm and filler ratio 95% Mg and 5% Cr of optimal input parameters to obtain a maximum weld nugget hardness of 93 HV.

Acknowledgements

The Authors are grateful to the Technical Education Quality Improvement Programme (TEQIP-II, Proceeding No.:149/TEQIPII/2017) for providing the fund to carry out the research. Also, the Authors are grateful for the support rendered by the Government College of Technology, Coimbatore, India and the Institute of Materials Joining, Shandong University, Jinan, China.

Nomenclature

Symbols

C – Center distance between the holes, mm
F – Filler ratio, %
P – Plunge depth, mm
R – Rotational speed, rpm
W – Welding speed, mm/min

Acronyms

CCD – Central Composite Design
RSM – Response Surface Methodology

References

1. Thomas, WM, Nicholas, ED, Needham, JC, Murch, MG, Temple-Smith, P & Dawes, CJ (1993), Friction stir butt welding (The Welding Institute TWI), UK patent 9125978.8.
2. Mohammad Amin Bozorgzadeh & Mohd Hasbullah Idris (2015), 'Friction Stir Welding International', *Journal of Review in Life Sciences*, Vol. 5, pp. 72-75.
3. Je-Hyoung Cho, Myung-Hyun Kim & Jun-Woong Choi, 2014, 'FSW Properties of Aluminium alloy 5000/6000 for Small Boat', *Journal of Welding and Joining*, Vol. 32, No. 1, pp. 34-39.
4. DG Mohan,Gopi S, (2021), Influence of In-situ induction heated friction stir welding on tensile, microhardness, corrosion resistance and microstructural properties of martensitic steel. Engineering *Research Express*, 3(2). https://doi.org/10.1088/2631-8695/abfe1d
5. Gopi S, DG Mohan, (2021), Evaluating the Welding Pulses of Various Tool Profiles in Single-Pass Friction Stir Welding of 6082-T6 Aluminium Alloy. *Journal of Welding and Joining*, Vol. 39, No 39(3), pp. 284–294. https://doi.org/10.3345/kjp.2021.39.3.284
6. A.Sasikumar, S Gopi, Dhanesh G Mohan, (2019), Effect of Magnesium and Chromium Fillers on the Microstructure and Tensile strength of Friction Stir

Welded Dissimilar Aluminium Alloys, *Materials Research Express,* Vol. 6.
7. Kesharwani, RK, Panda, SK & Pal, SK (2014), 'Multi Objective Optimization of Friction Stir Welding Parameters for Joining of Two Dissimilar Thin Aluminium Sheets', *Procedia Materials Science*, Vol. 6, pp. 178–187.
8. R.W. Fonda, P.S. Pao, H.N. Jones, C.R. Feng, B.J. Connolly, A.J. Davenport, (2009), Microstructure, mechanical properties, and corrosion of friction stir welded Al 5456, *Material Science Engineering* , Vol. 519, pp.1-8.
9. Aditya R. Prabhukhot , (2015), Effect of Heat Treatment on Hardness and Corrosion Behavior of 6082-T6 Aluminium Alloy in Artificial Sea Water, *International Journal of Materials Science and Engineering*, Vol. 3, pp. 287-294
10. P H Shaha, VishveshBadhekab, (2016), An experimental investigation of temperature distribution and joint properties of Al 7075 T651 friction stir welded aluminium alloys, Procedia Technology, vol. 23, pp. 543 – 550.
11. H M Anil Kumar, V VenkataRamana, MayurPawar, (2018), Experimental Study on Dissimilar Friction Stir welding of Aluminium Alloys (5083-H111 and 6082-T6) to investigate the mechanical properties, *Materials Science and Engineering*, Vol. 330.
12. H. S. Patil1, S. N. Soman, (2014), Corrosion Behaviour of Friction Stir Welded Aluminium Alloys AA6082-T6, American *Journal of Materials Engineering and Technology*, Vol. 2, pp. 29-33.
13. DG Mohan, Gopi S, Rajasekar V, (2018), Effect of induction heated friction stir welding on corrosive behaviour, mechanical properties and microstructure of AISI 410 stainless steel. *Indian Journal of Engineering and Materials Sciences*, Vol. 25, No. 3, pp. 203-208.
14. Jae-HyungChoa.b,Won Jae Kima, Chang Gil Leea, (2014), Evolution of microstructure and mechanical properties during friction stir welding of A5083 and A6082*, Procedia Engineering*, Vol. 81, pp. 2080-2085.
15. Dhanesh G. Mohan. And Gopi S., (2018). Induction assisted friction stir welding: a review, *Australian Journal of Mechanical Engineering*, Vol. 18, No.1, pp.119-123.
16. A. Silva-Magalhaes, J. De Backer, J. Martin, G. Bolmsjo, (2019), In-situ temperature measurement in friction stir welding of thick section aluminium alloys, *Journal of Manufacturing Processes*, Vol. 39, pp. 12-17.
17. Hwang Y-M, Kang Z-W, Chiou Y-C, Hsu H-H, (2008), Experimental study on temperature distributions within the workpiece during friction stir welding of aluminum alloys, *International Journal of Machine Tools and Manufacture,* Vol. 48, pp. 778-787.
18. Zhang Z, Liu YL, Chen JT, (2009), Effect of shoulder size on the temperature rise and the material deformation in friction stir welding, *International Journal of Advanced Manufacturing Technology*, Vol. 45, pp. 889-95.
19. Sakthivel T, Sengar GS, Mukhopadhyay J, (2009), Effect of welding speed on microstructure and mechanical properties of friction-stir-welded aluminum. *International Journal of Advanced Manufacturing Technology*, Vol. 43, pp. 468-73.
20. Dhanesh G. Mohan, Gopi, S., & Sasikumar, A., (2021). Examining the Mechanical and Metallurgical Properties of Single Pass Friction Stir Welded Dissimilar Aluminium Alloys Tee Joints. *SVOA Materials Science &Technology*, Vol. 3, No. 1, pp.6–12.
21. Dhanesh G. Mohan, S. Gopi, V.Rajasekar, (2018), Mechanical and corrosion resistance properties of hybrid-welded stainless steel, *Materials Performance*, Vol. 57.
22. Hatamleh O, Singh PM, Garmestani H, (2009), Corrosion susceptibility of peened friction stir welded 7075 aluminumalloy joints, *Corrosion Science*, Vol. 51, pp. 135-43.
23. Rafi HK, Ram GDJ, Phanikumar G, Rao KP, (2010), Microstructure and tensile properties of friction welded aluminium alloy AA7075-T6, *Materials & Design*, Vol. 31, pp. 2375-2380.
24. Mohan D.G., Tomków J., Gopi S. (2021) Induction assisted hybrid Friction Stir Welding of dissimilar materials AA5052 aluminium alloy and X12Cr13 stainless steel. *Advances in Materials Science*, Vol. 21, issue 3, in press.
25. Je-Hyoung Cho, Myung-Hyun Kim & Jun-Woong Choi, (2014), FSW Properties of Aluminium alloy 5000/6000 for Small Boat, *Journal of Welding and Joining*, vol. 32, no. 1, pp. 34-39.

Biographical notes

Sasikumar A. received his M.Tech degree in Advanced Manufacturing from SASTRA University, Thanjavur, Tamilnadu, India and next Ph.D., degree in Faculty of Mechanical Engineering from Anna University, Chennai, in 2006 and 2020, respectively. Since 2013, he has been working in the Department of Production Engineering at Government College of Technology, Coimbatore where currently he works as an assistant professor. His scientific interests focus on friction stir welding and friction stir processing. He has participated in 3 international conferences, published 10 scientific papers in international journals, as well as conference proceedings.

Gopi S. received his M.E degree in Engineering Design and Ph.D., degree in Faculty of Mechanical Engineering from Anna University, Chennai, in 2007 and 2013, respectively. Since 2006, he has been working in the Department of Production Engineering at Government College of Technology, Coimbatore where currently he works as an associate professor. His scientific interests focus on friction stir welding, production engineering and friction stir processing. He has participated in 10 international and national conferences, published 27 scientific papers in international journals, as well as conference proceedings.

Dhanesh G. Mohan received his M.E degree in Manufacturing Engineering and Ph. D. degree in the Faculty of Mechanical Engineering from Anna University, Chennai, in 2014 and 2019, respectively. Since 2019, he has been working in the Institute of Materials Joining, Shandong University, Jinan, China, where currently he works as a postdoctoral research fellow. His scientific interests focus on friction stir welding, additive manufacturing, high entropy alloys and friction stir processing. He has participated in 7 international conferences, published 22 scientific papers in international journals, as well as conference proceedings.